Phys. Lett. B 850 (2024) 138501

Contents lists available at ScienceDirect

Physics Letters B

journal homepage: www.elsevier.com/locate/physletb

Letter

Classes of complete dark photon models constrained by Z-physics

Miguel P. Bento [a], Howard E. Haber [b,*], João P. Silva [a]

[a] CFTP, Departamento de Física, Instituto Superior Técnico, Universidade de Lisboa, Avenida Rovisco Pais 1, Lisboa 1049, Portugal
[b] Santa Cruz Institute for Particle Physics, University of California, 1156 High Street, Santa Cruz, CA 95064, USA

ARTICLE INFO

Editor: J. Hisano

Keywords:
Dark photon
Dark matter
Precision electroweak physics

ABSTRACT

Dark Matter models that employ a vector portal to a dark sector are usually treated as an effective theory that incorporates kinetic mixing of the photon with a new U(1) gauge boson, with the Z boson integrated out. However, a more complete theory must employ the full $\mathrm{SU}(2)_L\times \mathrm{U}(1)_Y\times \mathrm{U}(1)_{Y'}$ gauge group, in which kinetic mixing of the Z boson with the new U(1) gauge boson is taken into account. The importance of the more complete analysis is demonstrated by an example where the parameter space of the effective theory that yields the observed dark matter relic density is in conflict with a suitably defined electroweak ρ parameter that is deduced from a global fit to Z physics data.

1. Introduction

The Standard Model (SM) of electroweak interactions based on an $\mathrm{SU}(2)_L\times \mathrm{U}(1)_Y$ gauge theory describes to very high precision the fundamental particles discovered in the laboratory [1]. Yet, it is known from cosmological and astrophysical observables, that SM particles constitute only around 15% of the total matter content of the Universe, with the remaining 85% consisting of non-baryonic dark matter (DM) that cannot be accommodated by the SM [2–4]. Some of the leading contenders for physics beyond the SM that contain candidates for particles that can contribute to the DM include models where the usual massless electromagnetic photon, associated with the unbroken $\mathrm{U}(1)_{\mathrm{EM}}$ gauge group, couples through kinetic mixing [5–9] with a very light massive dark photon [10] (also called dark Z' boson [11,12]) that is associated with a new $\mathrm{U}(1)_{Y'}$ gauge symmetry. The dark photon (or equivalently the dark Z' boson) serves as a mediator between the sector of SM particles and a dark sector which contains particles that are neutral with respect to SM gauge group. The DM can then be identified with either stable particles and/or particles with lifetimes significantly larger than the age of the Universe that reside in the dark sector (e.g., see [13–33]). This analysis can and is usually made without referring to the Z boson. The idea is that the interactions relevant for DM studies occur at an energy significantly below the Z boson mass (m_Z), in which case this field can be integrated out. One then proceeds to study the effective theory that depends solely on two parameters.

However, a complete electroweak and DM model must indeed start from the full $\mathrm{SU}(2)_L\times \mathrm{U}(1)_Y\times \mathrm{U}(1)_{Y'}$ gauge theory. The physical Z boson field will then comprise a small component of the $\mathrm{U}(1)_{Y'}$ boson field, which affects the interpretation of the precision electroweak observables measured at colliders. Now the question arises: in such complete theories, is there a tension between the parameters required for a (low-energy) explanation for DM and those required to conform with Z boson observables? A number of Z physics observables have been considered in [11,17,19,23,32–35]. In this work, we examine tree-level corrections to the electroweak ρ parameter, which is very precisely determined in [36]. This yields a very important condition that the putative complete electroweak-DM model must obey in order to comply with both dark matter searches and the collider constraints arising from precision electroweak studies.

In Section 2, we review the $\mathrm{SU}(2)_L\times \mathrm{U}(1)_Y\times \mathrm{U}(1)_{Y'}$ gauge theory, which includes kinetic mixing between the $\mathrm{U}(1)_Y$ and $\mathrm{U}(1)_{Y'}$ gauge bosons, where the gauge bosons are coupled to an arbitrary set of scalar multiplets. Diagonalizing the neutral vector boson squared mass matrix yields the photon, Z boson, and the dark Z' boson. Following [37], we define a suitable electroweak ρ parameter and show that the SM tree-level result of $\rho=1$ is modified. In Section 3, a dark matter candidate is introduced by adding a Dirac fermion χ to the model that is neutral with respect to the SM but has a nonzero $\mathrm{U}(1)_{Y'}$ charge. Two different mass orderings for m_χ and $m_{Z'}$ are considered. Conditions are then obtained on the model parameters such that χ constitutes the observed dark matter. In Section 4, we provide an example where the latter result is in conflict with the value of ρ deduced from a global fit to Z physics data. In particular, as noted in our conclusions presented in Section 5, realistic models containing a dark Z' as a vector portal to a dark sector

* Corresponding author.
E-mail addresses: miguelfilipebento@gmail.com (M.P. Bento), haber@scipp.ucsc.edu (H.E. Haber), jpsilva@cftp.ist.utl.pt (J.P. Silva).

https://doi.org/10.1016/j.physletb.2024.138501
Received 15 December 2023; Received in revised form 13 January 2024; Accepted 27 January 2024
Available online 2 February 2024

must be reconsidered in the framework of a gauge theory that contains the Z boson in addition to the photon and dark Z'. Ultimately, one must check all constraints imposed by the precision electroweak data in order to achieve a consistent DM model.

2. An extra vector boson

2.1. Gauge sector

The presence of an extra vector boson $\hat{X}$ allows for kinetic mixing between abelian gauge bosons in the Lagrangian,

$$\mathcal{L} \supset -\frac{1}{4}\hat{B}_{\mu\nu}\hat{B}^{\mu\nu} - \frac{1}{4}\hat{X}_{\mu\nu}\hat{X}^{\mu\nu} + \frac{\epsilon}{2c_W}\hat{X}_{\mu\nu}\hat{B}^{\mu\nu}\,, \tag{1}$$

where $\hat{B}_\mu$ and $\hat{X}_\mu$ are the gauge bosons of $U(1)_Y$ and $U(1)_{Y'}$, respectively, and $\hat{B}^{\mu\nu}$ and $\hat{X}^{\mu\nu}$ are the corresponding field strength tensors. The last term describes kinetic mixing between the $\mathrm{U}(1)_Y$ and the $\mathrm{U}(1)_{Y'}$ gauge bosons, where c_W is defined implicitly in Eq. (8) below.

Next, we transform the $\hat{B}$ and $\hat{X}$ fields such that

$$\hat{X}^\mu = \eta X^\mu\,, \quad \hat{B}^\mu = B^\mu + \frac{\epsilon}{c_W}\eta X^\mu\,, \tag{2}$$

where

$$\eta \equiv \frac{1}{\sqrt{1-\epsilon^2/c_W^2}}\,. \tag{3}$$

We then recover the canonical form of the kinetic Lagrangian, $\mathcal{L} \supset -\frac{1}{4}B_{\mu\nu}B^{\mu\nu} - \frac{1}{4}X_{\mu\nu}X^{\mu\nu}$. Adding to this the kinetic Lagrangian of the $\mathrm{SU}(2)_L$ fields ($W^\pm$ and W^3) and defining the $\mathrm{SU}(2)_L$, $\mathrm{U}(1)_Y$ and $\mathrm{U}(1)_{Y'}$ gauge couplings by g, g', and g_X, respectively, one can derive the mass eigenstates of the gauge bosons.

2.2. Scalar multiplets

All gauge bosons are massless before spontaneous gauge symmetry breaking. In order to generate mass for the Z boson and a very light dark photon (henceforth denoted as the dark Z'), one needs to break the gauge symmetry with some scalar fields. Here, we consider a complex scalar doublet Φ with $Y'=0$ and SM quantum numbers (i.e., weak isospin $t_1 = 1/2$ and hypercharge $y_1 = 1/2$), and $N-1$ additional real or complex scalar multiplets φ_i (the latter charged under $\mathrm{SU}(2)_L$, Y, and/or Y' with corresponding weak isospin t_i and U(1) charges y_i and y'_i, respectively, for $i=2,\ldots,N$), each with an electrically neutral component. The neutral components of the scalars acquire vacuum expectation values $\langle\Phi^0\rangle = v_1/\sqrt{2}$ and $\langle\varphi_i^0\rangle = v_i/\sqrt{2}$, $i=2,\ldots N$, which spontaneously break the gauge group. These, in turn, give mass to the $W^\pm$ boson such that

$$m_W^2 = \frac{g^2v^2}{4} = \frac{g^2\left[v_1^2 + \sum_{i=2}^N 2(C_{R_i} - y_i^2)v_i^2 c_i\right]}{4}\,, \tag{4}$$

where $C_{R_i} = t_i(t_i+1)$ for a complex [real] φ_i multiplet, with $c_i = 1$ [$c_i = 1/2$]. In order to approximately reproduce the observed value of m_W/m_Z, we shall choose scalar field multiplets such that

$$C_{R_i} = 3y_i^2\,, \tag{5}$$

which ensures that Eq. (16) is satisfied.

As for the neutral gauge bosons, by mixing B_μ and W_μ^3 in the usual way, we identify the photon field A_μ (and the corresponding orthogonal field Z_μ^0) by

$$A_\mu = W_\mu^3 s_W + B_\mu c_W\,, \tag{6}$$

$$Z_\mu^0 = W_\mu^3 c_W - B_\mu s_W\,, \tag{7}$$

where $c_W \equiv \cos\theta_W$ and $s_W \equiv \sin\theta_W$. Eqs. (6) and (7) define the weak mixing angle θ_W such that $e = g s_W$ and $g' = g t_W$ (where $t_W \equiv s_W/c_W$). Indeed, we may define the weak mixing angle (at tree level) in terms of physical observables via [37],

$$s_W^2 = \frac{\pi\alpha_{\mathrm{EM}}}{\sqrt{2}G_F m_W^2}\,, \tag{8}$$

where G_F is the weak interaction Fermi constant and $\alpha_{\mathrm{EM}} \equiv e^2/(4\pi)$. Note that Eq. (8) can be applied both in the SM and in $\mathrm{U}(1)'$ extended gauge theories.

The squared-mass matrix of the remaining (massive) neutral gauge bosons with respect to the $\{Z^0, X\}$ basis is then given by

$$\mathcal{M}^2 = \begin{bmatrix} m_{Z^0}^2 & (\mathcal{M}^2)_{12} \\ (\mathcal{M}^2)_{12} & (\mathcal{M}^2)_{22} \end{bmatrix}, \tag{9}$$

where η is defined in Eq. (3), $\tau \equiv g_X/g$,

$$(\mathcal{M}^2)_{12} = -\frac{m_{Z^0}^2}{v^2}\left[4\eta t_W \epsilon \sum_{i=1}^N v_i^2 y_i^2 + 4\eta\tau c_W \sum_{i=2}^N v_i^2 y_i y'_i\right]\,, \tag{10}$$

and

$$m_{Z^0} \equiv \frac{gv}{2c_W} = \frac{m_W}{c_W}\,. \tag{11}$$

We are suppressing the explicit expression for $(\mathcal{M}^2)_{22}$, as it is not needed in what follows. Note that the interaction eigenstate field Z^0 does *not* correspond to the field of the experimentally observed Z boson since it is *not* a mass eigenstate field, and the mass of the Z (denoted below by m_Z) is *not* equal to m_{Z^0}.

The mass eigenstate fields Z and Z' are obtained via

$$\begin{pmatrix} Z^0 & X \end{pmatrix} \mathcal{M}^2 \begin{pmatrix} Z^0 \\ X \end{pmatrix} = \begin{pmatrix} Z & Z' \end{pmatrix} \begin{pmatrix} m_Z^2 & 0 \\ 0 & m_{Z'}^2 \end{pmatrix} \begin{pmatrix} Z \\ Z' \end{pmatrix}, \tag{12}$$

where $m_{Z'}$ is the mass of the dark Z' and

$$\begin{pmatrix} Z^0 \\ X \end{pmatrix} = \begin{pmatrix} \cos\alpha & -\sin\alpha \\ \sin\alpha & \cos\alpha \end{pmatrix} \begin{pmatrix} Z \\ Z' \end{pmatrix} \tag{13}$$

defines the mixing angle α. We may then extract the important relation,

$$m_{Z^0}^2 = m_Z^2\cos^2\alpha + m_{Z'}^2\sin^2\alpha\,. \tag{14}$$

In an $\mathrm{SU}(2)_L\times \mathrm{U}(1)_Y$ gauge theory, the choice of scalar multiplets that satisfy Eq. (5) has been imposed in order to ensure that the tree-level electroweak ρ parameter,

$$\rho \equiv \frac{m_W^2}{m_Z^2 c_W^2}, \tag{15}$$

satisfies $\rho = 1$ without resorting to a fine-tuning of the choice of scalar field vacuum expectation values. Examples include multi-Higgs doublet models (for a review see, e.g., [38]), or models with one doublet and one septet [39,40]. As shown in [37], in models with an $\mathrm{SU}(2)_L\times \mathrm{U}(1)_Y\times \mathrm{U}(1)_{Y'}$ gauge group, Eq. (5) enforces instead a new tree-level parameter

$$\rho' \equiv \frac{\rho}{1+\left(\dfrac{m_{Z'}^2}{m_Z^2} - 1\right)\sin^2\alpha} = 1\,, \tag{16}$$

where we have used Eq. (14). The role of ρ' in an $\mathrm{SU}(2)_L\times \mathrm{U}(1)_Y\times \mathrm{U}(1)_{Y'}$ gauge theory is analogous to the role of ρ in an $\mathrm{SU}(2)_L\times \mathrm{U}(1)_Y$ gauge theory.

Using Eq. (8), it is convenient to replace Eq. (15) with the following equivalent definition:

$$\rho \equiv \frac{2G_F m_W^4}{m_Z^2\left(2G_F m_W^2 - \sqrt{2}\pi\alpha_{\rm EM}\right)}\,. \tag{17}$$

In particular, Eq. (8) is a suitable definition in both $\mathrm{SU}(2)_L\times \mathrm{U}(1)_Y$ and in $\mathrm{SU}(2)_L\times \mathrm{U}(1)_Y\times \mathrm{U}(1)_{Y'}$ gauge theories, independently of how one chooses to define c_W. Finally, using Eq. (16) we arrive at

$$\rho - 1 = (r-1)\sin^2\alpha\,, \tag{18}$$

where

$$r \equiv \frac{m_{Z'}^2}{m_Z^2}\,, \tag{19}$$

and the magnitude of $\sin\alpha$ is controlled by $\left(\mathcal{M}^2\right)_{12}$. In particular,

$$\sin^2 2\alpha = \frac{4\left[(\mathcal{M}^2)_{12}\right]^2}{(m_Z^2 - m_{Z'}^2)^2}\,. \tag{20}$$

It is useful to eliminate $\sin\alpha$ in favor of the parameter r_{12}^2 defined below:

$$r_{12}^2 \equiv \left(\frac{(\mathcal{M}^2)_{12}}{m_{Z^0}^2}\right)^2 = \frac{(1-r)^2\sin^2\alpha\cos^2\alpha}{\left[1-(1-r)\sin^2\alpha\right]^2}\,. \tag{21}$$

Then,

$$\sin^2\alpha = \frac{1-r+2r_{12}^2 - \sqrt{(1-r)^2 - 4r\,r_{12}^2}}{2(1-r)(1+r_{12}^2)}\,. \tag{22}$$

Combining Eq. (18) with Eq. (22) yields,

$$\rho - 1 = \frac{-1+r-2r_{12}^2 + \sqrt{(1-r)^2 - 4r\,r_{12}^2}}{2(1+r_{12}^2)}\,, \tag{23}$$

which is a monotonically decreasing function of r_{12}. This fact will be instrumental in the results obtained in Section 4.

In the dark matter models considered in Sections 3 and 4, we shall assume that $0 < m_{Z'} < m_Z$ or equivalently $0 < r < 1$. Then Eq. (18) implies that $\rho - 1 < 0$. It is then convenient to use Eq. (23) to obtain r_{12}^2 as a function of r and ρ:

$$r_{12}^2 = \frac{(1-\rho)(\rho - r)}{\rho^2}\,. \tag{24}$$

3. Dark matter

A dark matter candidate is commonly included in the dark Z' model either by adding an inert scalar field or by adding an $\mathrm{SU}(2)_L\times \mathrm{U}(1)_Y$ singlet Dirac fermion with a nonzero $\mathrm{U}(1)_{Y'}$ charge. In what follows, we shall consider such a Dirac fermion, denoted by χ, as the dark matter candidate.

Thus, the dark Lagrangian is given by

$$\mathcal{L}_{\rm DM} = i\overline{\chi}\not{D}\chi - m_\chi\overline{\chi}\chi\,, \tag{25}$$

where the covariant derivative can be expanded as

$$D_\mu = \partial_\mu + i g_X Y'\eta(s_\alpha Z_\mu + c_\alpha Z'_\mu)\,, \tag{26}$$

with $s_\alpha \equiv \sin\alpha$, $c_\alpha \equiv \cos\alpha$, and η is defined in Eq. (3). We note the difference between Eq. (26) and the corresponding expressions given in [4,41]

$$D_\mu \overset{[4,41]}{\supset} \partial_\mu + i g_X Y' Z'_\mu\,. \tag{27}$$

The approximation in Eq. (27) requires two assumptions: (i) $\eta \approx 1$, and (ii) $c_\alpha \approx 1$. Note that the latter is not guaranteed to be true in all models even if $\epsilon = 0$. Indeed, by adding non-inert, non-singlet scalars to the theory, c_α is controlled by ϵ and g_X. Because g_X still needs to be significant to explain the correct abundance of DM, we may constrain (and perhaps exclude) models using precision electroweak observables, such as the ρ parameter as defined in Eq. (17).

The interaction term of the Z' boson with a SM fermion ψ is given by

$$\mathcal{L}_{\rm int} \supset -\frac{g}{2c_W}\overline{\psi}\gamma^\mu\left(g_V - g_A\gamma_5\right)\psi Z'_\mu\,, \tag{28}$$

where

$$g_V = \left(2Qs_W^2 - T_3\right)s_\alpha + \left(\eta t_W\epsilon\right)\left(2Q - T_3\right)c_\alpha\,, \tag{29}$$

$$g_A = -T_3 s_\alpha - \left(\eta t_W \epsilon\right)T_3 c_\alpha\,, \tag{30}$$

and $Q = T_3 + Y$. In [4], the authors employ

$$\mathcal{L}_{\rm int} \overset{[4]}{\supset} \overline{\psi}\gamma^\mu(-\epsilon\, e\, Q)\psi Z'_\mu\,, \tag{31}$$

in the small ϵ and small $m_{Z'}$ approximation. In particular, in the case of a scalar field that is neutral with respect to $\mathrm{SU}(2)_L\times \mathrm{U}(1)_Y$ and has a nonzero $\mathrm{U}(1)_{Y'}$ charge (treated in [37]), one obtains $s_\alpha \simeq -\eta t_W\epsilon$ and $c_\alpha \simeq 1$ after dropping terms of order $\mathcal{O}(\epsilon^2)$ and $\mathcal{O}(r)$. Inserting these results into Eqs. (28)–(30) reproduces Eq. (31).

In the following, we assume that the DM candidate χ is in thermal equilibrium in the early Universe. The velocity averaged cross section for $\overline{\chi}\chi$ annihilation is given by $\left\langle\sigma_{\chi\chi}v\right\rangle \simeq 2\times 10^{-26}$ cm^3 s^{-1} $\simeq 1.7\times 10^{-9}$ GeV^{-2} (the latter in natural units) for values of $m_\chi \gtrsim 10$ GeV [2], under the assumption that χ particles saturate the observed DM abundance today. As the Universe evolves and the temperature drops, a point is reached where the DM decouples from the thermal bath and it freezes out [3,4]. Freeze-out in the $\mathrm{U}(1)_{Y'}$ model considered above may be accessed through two main regimes which we now briefly consider—the characteristic and secluded regimes.

3.1. Freeze-out: characteristic regime

The characteristic regime corresponds to the mass ordering given by $m_{Z'} > m_\chi > m_e$, where the dominant annihilation mechanism is the s-channel scattering process $\overline{\chi}\chi \to Z'^* \to \bar{f}f$. Then, the velocity averaged annihilation cross section is given by [4]

$$\left\langle\sigma_{\chi\chi}v\right\rangle \overset{[4]}{\approx} \frac{m_\chi^2}{\pi m_{Z'}^4}\left(\epsilon e g_X Y'\right)^2\,, \tag{32}$$

under the assumption that $m_\chi \gg m_e$ and $m_{Z'} \gg m_\chi$. By assuming $Y' = 1$ (and correcting some minor misprints in [4]), we obtain the correct DM abundance with

$$\frac{1.7\times 10^{-9}}{\mathrm{GeV}^2} \overset{[4]}{\approx} \frac{0.038}{\mathrm{GeV}^2}\left(\frac{m_\chi}{0.01\,\mathrm{GeV}}\right)^2\left(\frac{0.1\,\mathrm{GeV}}{m_{Z'}}\right)^4(\epsilon\, g_X)^2\,, \tag{33}$$

which, after fixing the masses, yields a value for $\epsilon\, g_X$ in agreement with [42,43]. However, as there are contributions from both vector and axial interactions, a full model computation of Eq. (32) is needed, which is provided in Appendix A, to obtain a more precise result. When Eq. (32) is replaced by the expression obtained in Eq. (A.7), we find that the numerical result obtained in Eq. (33) is modified by a factor of order unity.

For models with a light Z' where $m_\chi < m_{Z'} < 10$ GeV, the characteristic regime is ruled out by the bound obtained in Fig. 46 of [2], which is derived from the cosmic microwave background (CMB) data.

3.2. Freeze-out: secluded regime

The secluded regime, which was advocated in [41] and explored further in [44], corresponds to the mass ordering $m_\chi > m_{Z'} > m_e$, where the dominant annihilation mechanism is $\overline{\chi}\chi \to Z'Z'$ via t-channel χ-exchange. In contrast to the characteristic regime, the CMB bound cited above does not rule out a light Z' for $m_\chi > 10$ GeV. The corresponding velocity averaged annihilation cross section is given by [4]

$$\left\langle \sigma_{\chi\chi} v \right\rangle \overset{[4]}{\approx} \frac{g_X^4 Y'^4}{8\pi m_\chi^2}\,, \tag{34}$$

under the assumption that $m_\chi \gg m_{Z'}$. Assuming again that $Y' = 1$, we obtain the correct DM abundance with

$$1.7 \times 10^{-9}\,\mathrm{GeV}^{-2} \overset{[4]}{\approx} 0.04\,\frac{g_X^4}{m_\chi^2}\,, \tag{35}$$

which, after fixing the mass m_χ, yields a value for g_X.

A more precise analysis that employs the full $\mathrm{SU}(2)_L \times \mathrm{U}(1)_Y \times \mathrm{U}(1)_{Y'}$ model will modify the results obtained above. Using Eq. (26), the results of Eqs. (34)–(35) are modified as follows:

$$\left\langle \sigma_{\chi\chi} v \right\rangle \approx \frac{g_X^4 \eta^4 c_\alpha^4 Y'^4}{8\pi m_\chi^2}\,, \tag{36}$$

$$1.7 \times 10^{-9}\,\mathrm{GeV}^{-2} \approx 0.04\,\frac{g_X^4 \eta^4 c_\alpha^4}{m_\chi^2}\,. \tag{37}$$

After fixing m_χ and $m_{Z'}$, we may constrain the values of g_X and ϵ [after employing Eq. (22), which determines the value of c_α]. In particular, even if $\epsilon \ll 1$, one cannot assume in general that $c_\alpha \simeq 1$.

4. Dark matter and the electroweak ρ parameter

By considering Z' as the vector portal to a dark sector, we may infer a relation between the dark matter relic density and the parameters g_X and ϵ. In Section 3 we saw that by fixing m_χ and $m_{Z'}$ we could constrain g_X and ϵ through Eq. (33) and Eq. (37). The secluded regime is largely independent of ϵ, and we will use this regime to provide the following instructive example.

Consider an $\mathrm{SU}(2)_L \times \mathrm{U}(1)_Y \times \mathrm{U}(1)_{Y'}$ model that possesses scalar multiplets φ_i beyond the SM Higgs doublet that are non-inert (i.e., $v_i \neq 0$) and charged under both $\mathrm{U}(1)_Y$ and $\mathrm{U}(1)_{Y'}$. In particular, we assume a parameter regime where $\epsilon \ll 1$ and $r = m_{Z'}^2/m_Z^2 \ll 1$. Using Eq. (22),

$$c_\alpha^2 = \frac{1}{1 + r_{12}^2} + \mathcal{O}(r)\,. \tag{38}$$

Eq. (9) then yields $r_{12}^2 = \left[(\mathcal{M}^2)_{12}\right]^2/m_{Z^0}^4 \sim g_X^2/g^2$, under the assumption that[1]

$$\frac{4c_W}{v^2} \sum_i y_i y_i' v_i^2 \sim \mathcal{O}(1)\,. \tag{39}$$

For example, if $m_\chi = 20\,\mathrm{GeV}$ then Eq. (37) yields

$$g_X \sim 0.0645\,. \tag{40}$$

As g_X becomes larger, so does r_{12}^2. Because Eq. (23) was determined to be a monotonically decreasing function with r_{12}^2, the quantity $\rho - 1$ gets more negative with larger r_{12}. Thus, a large g_X pushes towards a larger negative value of $\rho - 1$. An illustration of this effect is exhibited in Fig. 1. It can be seen that for $r \ll 1$, the contribution of r to $\rho - 1$ is small. Then, we may approximate Eq. (23) by

$$\rho - 1 = -\frac{r_{12}^2}{1 + r_{12}^2} + \mathcal{O}(r)\,. \tag{41}$$

Using $r_{12}^2 \sim g_X^2/g^2 \sim 2.34 g_X^2$, we end up with

$$\rho - 1 \sim -0.0096\,. \tag{42}$$

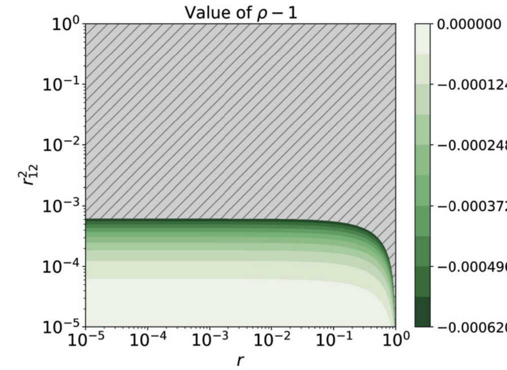

Fig. 1. Variation of $\rho - 1$ with r_{12}^2 and r obtained from Eq. (24). Note that $\rho - 1 < 0$ in light of Eq. (18). Values of $\rho - 1$ that are less than [more than] 5σ below the central value given in Eq. (43) (obtained in the global electroweak fit of [36]) are exhibited by the shaded green [gray hatched] regions of the plot.

This value, which lies in the gray hatched region of Fig. 1, is inconsistent with the global electroweak fit value of [36]

$$\rho_0 = 1.00038 \pm 0.00020\,. \tag{43}$$

Note that as defined by the authors in [36], $\rho_0 = 1$ exactly in the SM, and a deviation from $\rho_0 = 1$ can be interpreted as a consequence of new physics beyond the SM (under the assumption that it is a small perturbation that does not significantly affect other electroweak radiative corrections). In the present context, we can assume that the deviation from $\rho_0 = 1$ is due primarily to the tree-level effect exhibited in Eq. (23).

As a second example, consider an extended Higgs sector that contains an $\mathrm{SU}(2)_L \times \mathrm{U}(1)_Y$ singlet scalar φ with a $\mathrm{U}(1)_{Y'}$ charge of $y' = 1$. Eqs. (10) and (21) yield:

$$r_{12}^2 = \eta^2 t_W^2 \epsilon^2\,. \tag{44}$$

Under the assumption that $|\epsilon| \ll 1$ and $1 - r \sim \mathcal{O}(1)$, we can employ Eq. (23) to obtain:

$$\rho - 1 = \frac{r_{12}^2}{r - 1} + \mathcal{O}(r_{12}^4)\,. \tag{45}$$

After inserting Eq. (44) into the above result and noting that $\eta = 1 + \mathcal{O}(\epsilon^2)$ [cf. Eq. (3)], we end up with

$$\rho - 1 = -\frac{\epsilon^2 t_W^2}{1 - r} + \mathcal{O}(\epsilon^4)\,, \tag{46}$$

in agreement with a result previously obtained in [37]. For example, assuming that the true value of ρ_0 is no more than 5σ below the central value given in Eq. (43), one can deduce an upper limit of $|\epsilon| \lesssim 0.046$. This is one of a number of experimental observables that can be used to constrain the value of ϵ (e.g., see Fig. 6 of [44]).

Finally, we remark that in contrast to the dark matter models considered in Section 3, in models of asymmetric dark matter, the cross section required to annihilate the symmetric component of the dark matter must be roughly 2–3 times larger than the corresponding annihilation cross sections of symmetric thermal dark matter models [48,49]. The more efficient annihilation cross section required by asymmetric dark matter models implies a larger value of g_X, which would yield an even smaller allowable parameter space in light of Eq. (37).

5. Discussion and conclusions

In gauge theories with an $\mathrm{SU}(2)_L \times \mathrm{U}(1)_Y \times \mathrm{U}(1)_{Y'}$ gauge group, we have examined models whose low energy behavior appears to be equivalent to a model of a photon that mixes with a new light neutral gauge boson (e.g., the dark photon). In the literature, the latter is often employed in models that propose to explain the observed DM relic

[1] Note that the assumption that Eq. (39) is satisfied can be consistent with the requirement that there exists a SM-like Higgs boson h in the scalar spectrum (as indicated by the LHC Higgs data [45,46]) if the decoupling limit is realized [47] (where all new scalars beyond the SM are significantly heavier than h).

density, without considering the impact of the full SU(2)$_L\times$ U(1)$_Y\times$ U(1)$_{Y'}$ model on Z physics observables. It is remarkable that the implications of the ρ parameter alone considered in Section 4 provide a simple illustration that the two requirements—the origin of the DM and the consistency with Z physics observables—can easily be at odds with each other.

Additional constraints will arise when the impact of the SU(2)$_L\times$ U(1)$_Y\times$ U(1)$_{Y'}$ gauge theory on other precision electroweak observables is considered. For example, three tree-level shifts to the SM electroweak Lagrangian due to the effect of the mixing of the interaction eigenstates Z^0 and X are identified in [33], which are denoted by Δ_1, Δ_2, and Δ_3. In particular, Δ_1 is related to the tree-level ρ parameter via $\rho=(1+\Delta_1)^{-1}$. The other two quantities Δ_2 and Δ_3 correspond to shifts of the SM neutral current and the electromagnetic current to the physical Z boson, respectively. Indeed, there have been a number of authors (e.g., see [11,17,19,23,32–35]) who have performed fits to the precision electroweak data as a way of deducing interesting constraints on dark photon (dark Z) models. It would be of interest to generalize such studies to examine the full impact of the SU(2)$_L\times$ U(1)$_Y\times$ U(1)$_{Y'}$ gauge theory. One such approach is to employ an effective field theory technique that includes all the gauge boson fields of the SU(2)$_L\times$ U(1)$_Y\times$ U(1)$_{Y'}$ model (e.g., see [50]). We shall explore the implications of a more complete analysis in a future publication.

Declaration of competing interest

The authors declare the following financial interests/personal relationships which may be considered as potential competing interests:

Howard Haber reports financial support was provided by US Department of Energy. João Silva and Miguel Bento report financial support was provided by the Portuguese Fundação para a Ciência e Tecnologia.

Data availability

No data was used for the research described in the article.

Acknowledgements

We are grateful for discussions with Hooman Davoudiasl and Stefania Gori. The work of M.P.B. is supported in part by the Portuguese Fundação para a Ciência e Tecnologia (FCT) under contract SFRH/BD/146718/2019. The work of M.P.B. and J.P.S. is supported in part by FCT under Contracts CERN/FIS-PAR/0008/2019, PTDC/FIS-PAR/29436/2017, UIDB/00777/2020, and UIDP/00777/2020; these projects are partially funded through POCTI (FEDER), COMPETE, QREN, and the EU. The work of H.E.H. is supported in part by the U.S. Department of Energy Grant No. DE-SC0010107. H.E.H. is grateful for the hospitality and support during his visit to the Instituto Superior Técnico, Universidade de Lisboa, where their work was initiated.

Appendix A. The annihilation cross section in the characteristic regime revisited

In [4], the authors derive the cross section for dark matter annihilation in the characteristic regime. There is a misprint in the equation that when corrected takes the form

$$\sigma_{\chi\chi} \overset{[4]}{=} \frac{(\epsilon e g_X Y')^2}{12\pi s}\frac{\left(s+2m_\chi^2\right)\left(s+2m_e^2\right)}{(s-m_{Z'}^2)^2+m_{Z'}^2\Gamma_{Z'}^2}\frac{\beta_f}{\beta_i}\,, \tag{A.1}$$

where

$$\beta_i=\sqrt{1-\frac{4m_\chi^2}{s}} \quad\text{and}\quad \beta_f=\sqrt{1-\frac{4m_e^2}{s}}\,. \tag{A.2}$$

With the relative velocity v defined as $v=2\beta_i$, we may compute the velocity averaged annihilation cross section using Eq. (A.1),

$$\left\langle \sigma_{\chi\chi} v\right\rangle \overset{[4]}{=} \frac{(\epsilon e g_X Y')^2}{2\pi}\frac{\sqrt{m_\chi^2-m_e^2}\left(2m_\chi^2+m_e^2\right)}{m_\chi\left(m_{Z'}^2-4m_\chi^2\right)^2}\,, \tag{A.3}$$

where we have assumed $\Gamma_{Z'}/m_{Z'}\ll 1$. Eq. (A.3) can be further simplified under the assumption that $m_\chi\gg m_e$ and $m_{Z'}\gg m_\chi$, which yields the approximate result,

$$\left\langle \sigma_{\chi\chi} v\right\rangle \overset{[4]}{\approx} \frac{m_\chi^2}{\pi m_{Z'}^4}\left(\epsilon e g_X Y'\right)^2\,, \tag{A.4}$$

in agreement with Eq. (32).

In the full SU(2)$_L\times$ U(1)$_Y\times$ U(1)$_{Y'}$ model, we obtain the following expressions for the annihilation cross section and corresponding velocity averaged cross section:

$$\begin{aligned}\sigma_{\chi\chi} =& \frac{1}{12\pi s}\left(\frac{g\,g_X}{2c_W}\eta c_\alpha Y'\right)^2\frac{s+2m_\chi^2}{(s-m_{Z'}^2)^2+m_{Z'}^2\Gamma_{Z'}^2}\times \\ & \left[g_V^2(s+2m_e^2)+g_A^2(s-4m_e^2)\right]\frac{\beta_f}{\beta_i}\,,\end{aligned} \tag{A.5}$$

and

$$\begin{aligned}\left\langle \sigma_{\chi\chi} v\right\rangle =& \frac{1}{2\pi}\left(\frac{g\,g_X}{2c_W}\eta c_\alpha Y'\right)^2\times \\ & \frac{\sqrt{m_\chi^2-m_e^2}\left[2m_\chi^2(g_V^2+g_A^2)+m_e^2(g_V^2-2g_A^2)\right]}{m_\chi\left(m_{Z'}^2-4m_\chi^2\right)^2}\,,\end{aligned} \tag{A.6}$$

in agreement with Eq. (4.1) of [22] in the absence of an axial vector coupling of the DM to the Z'. By using the same set of approximations, $m_\chi\gg m_e$ and $m_{Z'}\gg m_\chi$, employed in the derivation of Eq. (A.4), we obtain the thermally averaged annihilation cross section,

$$\left\langle \sigma_{\chi\chi} v\right\rangle \approx \frac{m_\chi^2}{\pi m_{Z'}^4}(g_V^2+g_A^2)\left(\frac{g\,g_X}{2c_W}\eta c_\alpha Y'\right)^2\,, \tag{A.7}$$

which yields an $\mathcal{O}(1)$ correction to the result quoted in Eq. (32).

References

[1] Y. Grossman, Y. Nir, The Standard Model: From Fundamental Symmetries to Experimental Tests, Princeton University Press, Princeton, NJ, 2023, https://press.princeton.edu/books/hardcover/9780691239101/the-standard-model.

[2] N. Aghanim, et al., Planck 2018 results. VI. Cosmological parameters, Astron. Astrophys. 641 (2020) A6, https://doi.org/10.1051/0004-6361/201833910, arXiv:1807.06209, Erratum: Astron. Astrophys. 652 (2021) C4.

[3] S. Profumo, An Introduction to Particle Dark Matter, World Scientific, Singapore, 2017, https://doi.org/10.1142/q0001.

[4] M. Bauer, T. Plehn, Yet Another Introduction to Dark Matter: The Particle Physics Approach, Lecture Notes in Physics, vol. 959, Springer Nature, Cham, Switzerland, 2019, https://link.springer.com/book/10.1007/978-3-030-16234-4.

[5] L.B. Okun, Limits of electrodynamics: paraphotons?, Sov. Phys. JETP 56 (1982) 502, http://jetp.ras.ru/cgi-bin/dn/e_056_03_0502.pdf.

[6] P. Galison, A. Manohar, Two Z's or not two Z's?, Phys. Lett. B 136 (1984) 279–283, https://doi.org/10.1016/0370-2693(84)91161-4.

[7] B. Holdom, Two U(1)'s and Epsilon Charge Shifts, Phys. Lett. B 166 (1986) 196–198, https://doi.org/10.1016/0370-2693(86)91377-8.

[8] R. Foot, X.-G. He, Comment on Z–Z' mixing in extended gauge theories, Phys. Lett. B 267 (1991) 509–512, https://doi.org/10.1016/0370-2693(91)90901-2.

[9] K.S. Babu, C.F. Kolda, J. March-Russell, Implications of generalized Z–Z' mixing, Phys. Rev. D 57 (1998) 6788–6792, https://doi.org/10.1103/PhysRevD.57.6788, arXiv:hep-ph/9710441.

[10] R. Essig, P. Schuster, N. Toro, B. Wojtsekhowski, An Electron Fixed Target Experiment to Search for a New Vector Boson A' Decaying to e^+e^-, J. High Energy Phys. 02 (2011) 009, https://doi.org/10.1007/JHEP02(2011)009, arXiv:1001.2557.

[11] H. Davoudiasl, H.-S. Lee, W.J. Marciano, "Dark" Z implications for Parity Violation, Rare Meson Decays, and Higgs Physics, Phys. Rev. D 85 (2012) 115019, https://doi.org/10.1103/PhysRevD.85.115019, arXiv:1203.2947.

[12] A. Alves, S. Profumo, F.S. Queiroz, The dark Z' portal: direct, indirect and collider searches, J. High Energy Phys. 04 (2014) 063, https://doi.org/10.1007/JHEP04(2014)063, arXiv:1312.5281.

[13] N. Arkani-Hamed, N. Weiner, LHC Signals for a SuperUnified Theory of Dark Matter, J. High Energy Phys. 12 (2008) 104, https://doi.org/10.1088/1126-6708/2008/12/104, arXiv:0810.0714.

[14] L. Ackerman, M.R. Buckley, S.M. Carroll, M. Kamionkowski, Dark Matter and Dark Radiation, Phys. Rev. D 79 (2009) 023519, https://doi.org/10.1103/PhysRevD.79.023519, arXiv:0810.5126.

[15] J.L. Feng, M. Kaplinghat, H. Tu, H.-B. Yu, Hidden Charged Dark Matter, J. Cosmol. Astropart. Phys. 07 (2009) 004, https://doi.org/10.1088/1475-7516/2009/07/004, arXiv:0905.3039.

[16] X. Chu, T. Hambye, M.H.G. Tytgat, The Four Basic Ways of Creating Dark Matter Through a Portal, J. Cosmol. Astropart. Phys. 05 (2012) 034, https://doi.org/10.1088/1475-7516/2012/05/034, arXiv:1112.0493.

[17] H. Davoudiasl, H.-S. Lee, W.J. Marciano, Muon Anomaly and Dark Parity Violation, Phys. Rev. Lett. 109 (2012) 031802, https://doi.org/10.1103/PhysRevLett.109.031802, arXiv:1205.2709.

[18] R. Foot, S. Vagnozzi, Dissipative hidden sector dark matter, Phys. Rev. D 91 (2015) 023512, https://doi.org/10.1103/PhysRevD.91.023512, arXiv:1409.7174.

[19] D. Curtin, R. Essig, S. Gori, J. Shelton, Illuminating Dark Photons with High-Energy Colliders, J. High Energy Phys. 02 (2015) 157, https://doi.org/10.1007/JHEP02(2015)157, arXiv:1412.0018.

[20] R. Foot, S. Vagnozzi, Diurnal modulation signal from dissipative hidden sector dark matter, Phys. Lett. B 748 (2015) 61–66, https://doi.org/10.1016/j.physletb.2015.06.063, arXiv:1412.0762.

[21] H. An, M. Pospelov, J. Pradler, A. Ritz, Direct Detection Constraints on Dark Photon Dark Matter, Phys. Lett. B 747 (2015) 331–338, https://doi.org/10.1016/j.physletb.2015.06.018, arXiv:1412.8378.

[22] A. Alves, A. Berlin, S. Profumo, F.S. Queiroz, Dark Matter Complementarity and the Z′ Portal, Phys. Rev. D 92 (8) (2015) 083004, https://doi.org/10.1103/PhysRevD.92.083004, arXiv:1501.03490.

[23] H. Davoudiasl, H.-S. Lee, W.J. Marciano, Low Q^2 weak mixing angle measurements and rare Higgs decays, Phys. Rev. D 92 (5) (2015) 055005, https://doi.org/10.1103/PhysRevD.92.055005, arXiv:1507.00352.

[24] M. Backovic, A. Mariotti, D. Redigolo, Di-photon excess illuminates Dark Matter, J. High Energy Phys. 03 (2016) 157, https://doi.org/10.1007/JHEP03(2016)157, arXiv:1512.04917.

[25] R. Foot, S. Vagnozzi, Solving the small-scale structure puzzles with dissipative dark matter, J. Cosmol. Astropart. Phys. 07 (2016) 013, https://doi.org/10.1088/1475-7516/2016/07/013, arXiv:1602.02467.

[26] F.C. Correia, S. Fajfer, Restrained dark $U(1)_d$ at low energies, Phys. Rev. D 94 (11) (2016) 115023, https://doi.org/10.1103/PhysRevD.94.115023, arXiv:1609.00860.

[27] S. Knapen, T. Lin, K.M. Zurek, Light Dark Matter: Models and Constraints, Phys. Rev. D 96 (11) (2017) 115021, https://doi.org/10.1103/PhysRevD.96.115021, arXiv:1709.07882.

[28] L. Darmé, S. Rao, L. Roszkowski, Light dark Higgs boson in minimal sub-GeV dark matter scenarios, J. High Energy Phys. 03 (2018) 084, https://doi.org/10.1007/JHEP03(2018)084, arXiv:1710.08430.

[29] P. Ilten, Y. Soreq, M. Williams, W. Xue, Serendipity in dark photon searches, J. High Energy Phys. 06 (2018) 004, https://doi.org/10.1007/JHEP06(2018)004, arXiv:1801.04847.

[30] C. Mondino, M. Pospelov, J.T. Ruderman, O. Slone Dark Higgs Dark Matter, Phys. Rev. D 103 (3) (2021) 035027, https://doi.org/10.1103/PhysRevD.103.035027, arXiv:2005.02397.

[31] A.L. Foguel, G.M. Salla, R.Z. Funchal, (In)Visible signatures of the minimal dark abelian gauge sector, J. High Energy Phys. 12 (2022) 063, https://doi.org/10.1007/JHEP12(2022)063, arXiv:2209.03383.

[32] K. Harigaya, E. Petrosky, A. Pierce, Precision Electroweak Tensions and a Dark Photon, arXiv:2307.13045, https://doi.org/10.48550/arXiv.2307.13045.

[33] H. Davoudiasl, K. Enomoto, H.-S. Lee, J. Lee, W.J. Marciano, Searching for new physics effects in future W mass and $\sin^2\theta_W(Q^2)$ determinations, Phys. Rev. D 108 (11) (2023) 115018, https://doi.org/10.1103/PhysRevD.108.115018, arXiv:2309.04060.

[34] A. Hook, E. Izaguirre, J.G. Wacker, Model Independent Bounds on Kinetic Mixing, Adv. High Energy Phys. 2011 (2011) 859762, https://doi.org/10.1155/2011/859762, arXiv:1006.0973.

[35] J. Sun, Z.-P. Xing, Dark photon effects with the kinetic and mass mixing in Z boson decay processes, arXiv:2310.06526, https://doi.org/10.48550/arXiv.2310.06526.

[36] J. Erler, A. Freitas, Electrowek Model and Constrains on New Physics, Chapter 10, in: The Review of Particle Physics, R. L. Workman et al. [Particle Data Group], in: Prog. Theor. Exp. Phys., vol. 2022, 2022, p. 083C01, https://doi.org/10.1093/ptep/ptac097, https://pdg.lbl.gov/2023/reviews/rpp2023-rev-standard-model.pdf.

[37] M.P. Bento, H.E. Haber, J.P. Silva, Tree-level Unitarity in $\mathrm{SU}(2)_L\times\mathrm{U}(1)_Y\times\mathrm{U}(1)_{Y'}$ Models, J. High Energy Phys. 10 (2023) 083, https://doi.org/10.1007/JHEP10(2023)083, arXiv:2306.01836.

[38] G.C. Branco, P.M. Ferreira, L. Lavoura, M.N. Rebelo, M. Sher, J.P. Silva, Theory and phenomenology of two-Higgs-doublet models, Phys. Rep. 516 (2012) 1–102, https://doi.org/10.1016/j.physrep.2012.02.002, arXiv:1106.0034.

[39] S. Kanemura, M. Kikuchi, K. Yagyu, Probing exotic Higgs sectors from the precise measurement of Higgs boson couplings, Phys. Rev. D 88 (2013) 015020, https://doi.org/10.1103/PhysRevD.88.015020, arXiv:1301.7303.

[40] M.-J. Harris, H.E. Logan, Constraining the scalar septet model through vector boson scattering, Phys. Rev. D 95 (9) (2017) 095003, https://doi.org/10.1103/PhysRevD.95.095003, arXiv:1703.03832.

[41] M. Pospelov, A. Ritz, M.B. Voloshin, Secluded WIMP dark matter, Phys. Lett. B 662 (2008) 53–61, https://doi.org/10.1016/j.physletb.2008.02.052, arXiv:0711.4866.

[42] E. Izaguirre, G. Krnjaic, P. Schuster, N. Toro, Physics motivation for a pilot dark matter search at Jefferson Laboratory, Phys. Rev. D 90 (1) (2014) 014052, https://doi.org/10.1103/PhysRevD.90.014052, arXiv:1403.6826.

[43] H. Davoudiasl, W.J. Marciano, Running of the U(1) coupling in the dark sector, Phys. Rev. D 92 (3) (2015) 035008, https://doi.org/10.1103/PhysRevD.92.035008, arXiv:1502.07383.

[44] J.A. Evans, S. Gori, J. Shelton, Looking for the WIMP Next Door, J. High Energy Phys. 02 (2018) 100, https://doi.org/10.1007/JHEP02(2018)100, arXiv:1712.03974.

[45] G. Aad, et al., A detailed map of Higgs boson interactions by the ATLAS experiment ten years after the discovery, Nature 607 (7917) (2022) 52–59, https://doi.org/10.1038/s41586-022-04893-w, arXiv:2207.00092, Erratum: Nature 612 (2022) E24.

[46] A. Tumasyan, et al., A portrait of the Higgs boson by the CMS experiment ten years after the discovery, Nature 607 (7917) (2022) 60–68, https://doi.org/10.1038/s41586-022-04892-x, arXiv:2207.00043.

[47] J.F. Gunion, H.E. Haber, The CP conserving two Higgs doublet model: The Approach to the decoupling limit, Phys. Rev. D 67 (2003) 075019, https://doi.org/10.1103/PhysRevD.67.075019, arXiv:hep-ph/0207010.

[48] M.L. Graesser, I.M. Shoemaker, L. Vecchi, Asymmetric WIMP dark matter, J. High Energy Phys. 10 (2011) 110, https://doi.org/10.1007/JHEP10(2011)110, arXiv:1103.2771.

[49] H. Iminniyaz, M. Drees, X. Chen, Relic Abundance of Asymmetric Dark Matter, J. Cosmol. Astropart. Phys. 07 (2011) 003, https://doi.org/10.1088/1475-7516/2011/07/003, arXiv:1104.5548.

[50] J. Aebischer, W. Altmannshofer, E.E. Jenkins, A.V. Manohar, Dark matter effective field theory and an application to vector dark matter, J. High Energy Phys. 06 (2022) 086, https://doi.org/10.1007/JHEP06(2022)086, arXiv:2202.06968.